Fully-Decoupled Radio Access Networks: A Flexible Downlink Multi-Connectivity and Dynamic Resource Cooperation Framework

Kai Yu, *Student Member, IEEE*, Quan Yu, *Fellow, IEEE*, Zhixuan Tang, *Student Member, IEEE*, Jiwei Zhao, *Member, IEEE*, Bo Qian, *Member, IEEE*, Yunting Xu, *Student Member, IEEE*, Haibo Zhou, *Senior Member, IEEE*, and Xuemin Shen, *Fellow, IEEE*

***Abstract*— To enable flexible base stations (BS) association and dynamic resource management for personalized user equipment (UE) download service provision in the next-generation mobile communication network (6G), in this paper, we investigate the downlink (DL) transmission scenario in an origin fully-decoupled radio access network (FD-RAN) architecture. Considering the unique fully-decoupled UL/DL access feature, we propose an efficient two-stage DL channel estimation method in the FD-RAN. We formulate a novel multi-connectivity and dynamic resource cooperation problem with joint multiple-BS and multiple-UE association and coordinated beamforming, aiming at maximizing the weighted sum achievable rate in DL FD-RAN. By leveraging the many-to-many swap-matching theory and fractional relaxation approach, we solve the dynamic UE scheduling problem with multiple-BS and multiple-UE association and the coordinated beamforming problem, respectively. Extensive simulation results based on standard 3GPP 36.873 urban micro channel demonstrate that the proposed framework can improve the average spectral efficiency by 34.9% as compared to the traditional maximum ratio transmission beamforming method.**

***Index Terms*— Radio access network (RAN), channel estimation, many-to-many matching, coordinated beamforming, fractional programming (FP).**

Manuscript received 7 June 2022; revised 26 September 2022; accepted 5 November 2022. Date of publication 1 December 2022; date of current version 12 June 2023. This work was supported in part by the National Natural Science Foundation Original Exploration Project of China under Grant 62250004, in part by the National Natural Science Foundation of China under Grant 62271244, in part by the Natural Science Fund for Distinguished Young Scholars of Jiangsu Province under Grant BK20220067, and in part by the Natural Sciences and Engineering Research Council of Canada (NSERC). The associate editor coordinating the review of this article and approving it for publication was D. Niyato. *(Corresponding author: Haibo Zhou.)*

Kai Yu, Zhixuan Tang, Jiwei Zhao, and Yunting Xu are with the School of Electronic Science and Engineering, Nanjing University, Nanjing 210023, China (e-mail: kaiyu@smail.nju.edu.cn; zhixuantang@smail.nju.edu.cn; jw_zhao@smail.nju.edu.cn; yuntingxu@smail.nju.edu.cn).

Quan Yu and Haibo Zhou are with the School of Electronic Science and Engineering, Nanjing University, Nanjing 210023, China, and also with the Peng Cheng Laboratory, Shenzhen 518000, China (e-mail: yuquan61@qq.com; haibozhou@nju.edu.cn).

Bo Qian is with the Department of Mathematics and Theories, Peng Cheng Laboratory, Shenzhen 518000, China (e-mail: boqian@pcl.ac.cn).

Xuemin Shen is with the Department of Electrical and Computer Engineering, University of Waterloo, Waterloo, ON N2L 3G1, Canada (e-mail: sshen@uwaterloo.ca).

Color versions of one or more figures in this article are available at https://doi.org/10.1109/TWC.2022.3224010.

Digital Object Identifier 10.1109/TWC.2022.3224010

I. Introduction

THE last decade has seen a proliferation of new applications such as virtual reality (VR/AR), telemedicine, remote driving, and the massive internet of things (IoTs), each of them has specific requirements for uplink (UL) and downlink (DL) transmission rates, respectively [1], [2], [3], [4]. Currently, user equipments (UE) merely associate with the base station providing the largest DL received power [5]. Such solutions may have difficulties in meeting diverse UL/DL requirements of various applications [1]. Driven by the need for a customized user association, the UL/DL decoupled access technology has come out, which allows UEs to access different base stations for UL and DL communication independently in heterogeneous networks (HetNets) [6]. However, by managing UL/DL association independently, efficient resource management and network control turn out to be very challenging in the existing radio access networks (RAN).

To support more flexible base stations association and resource cooperation in the next generation mobile communication network (6G), an original RAN architecture, namely fully decoupled access RAN (FD-RAN) has been proposed [7]. In the FD-RAN architecture, the typical base stations (BSs) are essentially decoupled into three types of BSs, i.e., control BSs, UL BSs (UBSs), and DL BSs (DBSs). Through the physically decoupling architecture feature, the UL and DL transmission can be fully separated, which can allow the flexibly deploying UBSs and DBSs according to the UEs' service and coverage requirements. In addition, the collaboration of multiple BSs to provide personalized services for every UE has become the default operation mode in stand-alone UL and DL networks. FD-RAN has shown its potential in elastic multiple-BS and multiple-UE association and dynamic resource cooperation, which are also crucial to DL coordinated beamforming. The main idea of DL multi-BS multi-UE coordinated beamforming is regarding multiple BSs as one virtual BS and each UE can choose a subset of the total antennas in this virtual BS [8], [9], that is to say, multiple access points can simultaneously transmit data to one UE (e.g., cell-free multi-input multi-output, CF-MIMO) [10], [11]. As the control signaling of

each UE interacts with one certain BS, frequent signaling handover is inevitable, which may bring additional challenges to the quality of experience in DL communications [12]. The control BSs with wide coverage and physically independent control channels in FD-RAN will bring flexible signaling interaction to DL services, thereby supporting flexible access and data transmission to UEs. However, since the UL and DL experience different paths in FD-RAN, the appropriate channel state information (CSI) acquisition method is important. The traditional DL channel estimation is based on channel reciprocity. This technology can not be directly applied to the FD-RAN DL communications as both the UL and DL radio units are independently deployed.

Based on the above considerations, we formulate a DL multi-BS and multi-UE association and dynamic resource cooperation problem, aiming at maximizing the weighted sum achievable rate in FD-RAN. We first model the two-stage channel estimation error, i.e. the estimation error between DL pilot transmission and UL feedback. Secondly, we model the sum-rate maximizing problem as a mixed-integer non-convex programming. After that, this problem is decomposed into the multi-BS and multi-UE association sub-problem and beamforming sub-problem, respectively. Considering the realistic BS capacity limit and multi-connectivity nature in FD-RAN, we model it as a many-to-many matching game [13]. Note that the acquisition of matching relationships among multiple UEs usually requires frequent signaling interactions, which can be solved with the help of the physically independent control channels in FD-RAN. To get a stable matching, we introduce a swap-based many-to-many matching method [14]. Since the DL coordinated beamforming problem is non-convex which is hard to solve, we exploit a fractional-programming-based (FP) relaxation by introducing second-order relaxation variables to transform the problem into a linear optimization problem. After that, we further transform it into an unconstrained optimization problem using the Lagrangian dual method, and use alternating optimization to optimize beamforming. In particular, the contributions of this paper are listed as follows:

- We investigate a two-stage channel estimation in the DL FD-RAN, in which the DBSs first transmit DL pilots to UEs, then, each UE exploits the unquantized quadrature-amplitude modulation (QAM) to feed the measured channel state information, and the UL channel is estimated by the minimum mean square error (MMSE) estimator. This two-stage channel estimation considers the fully-decoupled DL/UL access feature and will efficiently estimate the DL CSI in the UL/DL fully decoupled access scenarios.
- We propose a swap-based many-to-many matching algorithm for the multi-BS and multi-UE association-oriented multi-connectivity problem in the DL FD-RAN. In the initialization phase, each UE accesses multiple DBSs based on the DL received power. In the swap-matching phase, every paired UEs can swap the associated BS index under the condition that the post-swap UE-DBS associations will not decrease the sum utility. Through iterative swap operations, this proposed algorithm can effectively improve the sum utility in DL FD-RAN, and it is proven to converge to a stable matching.
- We design an FP-based coordinated beamforming algorithm in the DL FD-RAN. The non-convex beamforming problem is transformed into a linear unconstrained optimization by introducing second-order relaxation variables and the Lagrangian dual method, and the beamforming of each BS can be independently calculated by the bisection search method, which can significantly improve the sum capacity in the FD-RAN.

The remainder of this paper is organized as follows. In Section II, we summarize the related works in three aspects. In Section III, we introduce the system model of FD-RAN architecture, model the DL signal, and propose the two-stage channel estimation. The optimization problem is formulated in Section IV. In Section V, we give the basic description of the many-to-many matching for UE association. In Section VI, the multi-connectivity problem is solved by the proposed swap-matching algorithm. Section VII introduces the DL coordinated beamforming algorithm. The extensive simulation results are presented in Section VIII. Finally, we draw the conclusion in Section IX.

II. Related Works

A. Evolution of UL/DL Association

RAN is a major component of wireless communication systems that can connect individual BSs to a centralized processing unit through wired/wireless fronthauls, which has supported multiple advanced applications [15], [16]. It can effectively boost the flexible configuration capabilities of wireless resources while reducing capital and operation costs. In the existing RAN architectures, both the UL and DL associations are dominated by the DL received power (RSRP). The recent developments of various applications may have different service requirements in UL and DL communications, which inspired researchers to redesign the uplink and DL access rules [2]. F. Boccardi et al. firstly proposed the UL/DL decoupled access under a HetNet [17]. Some literature showed that this flexible UL/DL association rule can bring significant capacity improvement to the UL and achieve load balancing [18], [19], [20]. Yu et al. investigated the UL/DL decoupled technology in C-V2X communications [18]. When UEs access different BSs in UL/DL, high-speed signaling exchanges and flexible data transmission are needed, which makes it challenging to be deployed in existing RAN architectures. To support more flexible UL/DL associations for diverse applications, Yu et al. proposed a more general FD-RAN architecture in which the physically independent UL, DL and control BSs were connected to a centralized edge cloud (EC) [7]. Whether it is in the FD-RAN architecture or the UL/DL decoupled technology, UEs access different radio units in UL and DL. The traditional channel estimation methods based on channel reciprocity are not suitable anymore [21]. Therefore, in FD-RAN architectures, the channel estimation should exploit the traditional DL training and UL feedback method [22].

Caire et al. analyzed the effects of DL pilots training, feedback, and channel estimation errors with the unquantized analog feedback method [23].

B. Matching Based UE Association

The matching theory is an effective mathematical tool that attempts to describe the formation of mutually beneficial relationships between different players, which is an efficient tool for analyzing and designing dynamic wireless network resources management [13]. Jorswieck first proposed stable matching for dynamic wireless resource allocation [24]. In addition, UE scheduling can be treated as a classical matching problem. Shen and Yu have exploited one-to-one matching for the UL single-connectivity [25]. In contrast to static matching [26], matching with a dynamic preference list which is called matching with externalities is more general in the interfered wireless environment (e.g., co-channel interference) [27]. In [14], two many-to-many matching game algorithms with externalities were designed to solve the UE-subchannel scheduling problem. Based on the initialization with preference lists and the two-side swap matching operations, the proposed matching algorithms were proved with exchange stability. Many-to-many matching for multi-connectivity in multi-BS, multi-UE systems were introduced in the comprehensive survey [28]. The one-to-one matching for the single-connectivity in multi-BS, multi-UE systems has been applied, however, authors have not discussed multi-connectivity in DL multi-BS, multi-UE coordinated beamforming problem in the proposed framework [25].

C. DL Coordinated Beamforming

The multi-UE MIMO (MU-MIMO) which enables simultaneous data transmission has shown remarkable performance improvements in network capacity. However, with the evolution of the network densification, many mobile UEs located at the cell boundary may suffer severe interference from other BSs. Therefore, efficiently coordinated beamforming is crucial in multicellular multi-UE MIMO networks. In [29], authors considered the DL intra-cell and inter-cell interference of a MIMO broadcast channel, then transformed the sum-rate maximizing problem as a weighted mean-square minimization problem solved by a sequential iteration algorithm. Shen and Yu proposed a second-order relaxation of the non-convex signal-to-interference-noise-ratio (SINR) [30], and developed a fractional programming (FP) based coordinated beamforming algorithm which outperformed the weighted mean square error beamforming in [29]. Focusing on transforming the interference into the desired signal, many frameworks such as network MIMO, distributed antennas, and CF-MIMO were widely investigated [31], [32]. Ammar et al. studied both coherent and non-coherent transmission in CF-MIMO [33]. To solve the joint UE scheduling and coordinated beamforming problem, a norm approximation and FP programming-based block coordinated decent algorithm was proposed. However, to get the MIMO CSI, most of these papers focused on exploiting channel reciprocity or angular reciprocity [31], [34], however, there is rare literature investigating the two-stage channel estimation error (i.e., DL training and UL feedback).

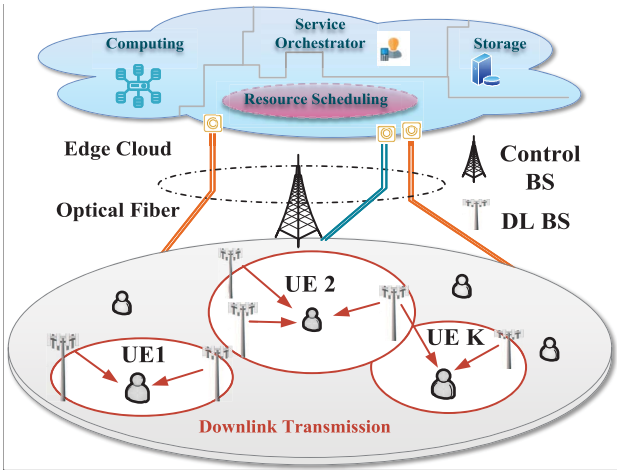

Fig. 1. Resource cooperation framework in DL FD-RAN.

Notation: Note that $\mathbb{E}$ represents the expectation, while $|\cdot|$ and $\|\cdot\|$ represent the Euclidean norms of scalar and vector, respectively. We denote the lower and upper case letters as scalars (e.g., b and B). Meanwhile, the bold letters denote the vectors or matrices. We also denote the operation $(\cdot)^{-1}$, $(\cdot)^{\dagger}$ as the inverse and conjugate transpose, respectively. $\mathbf{S} = \text{diag}(\mathbf{b})$ denotes the diagonal matrix constructed from the vector $\mathbf{b}$. For a set $\mathcal{E}$, $|\mathcal{E}|$ is denoted as the cardinality of this set.

III. System Model

In this section, we first introduce the network model of downlink FD-RAN architecture. After that, we present the signal model of the collaborative transmission. At last, the DL pilot transmission and feedback process are presented.

A. Network Model

In this paper, a new radio access network architecture called FD-RAN is illustrated in Fig. 1 with both control and DBSs connected to an EC via high-speed fronthauls [7]. We consider the EC has powerful signal processing capabilities for integrated signal processing, storage, and resource scheduling. This centralized setup enables multiple DBSs to collaboratively and simultaneously serve multiple UEs within the overlapping area. Assuming that there exists $\mathcal{M} = \{1, \ldots, M\}$ DBSs, and each BS is equipped with N antennas forming a linear array. We also assume there exists $\mathcal{K} = \{1, \ldots, K\}$ UEs, each is equipped with a single antenna.

Note that the DBSs' coverage areas are generally overlapping, we define the serving set for UE $k \in \mathcal{K}$ as $\mathcal{E}_k \subset \mathcal{M}$ which denotes BSs who serves this UE. Besides, these serving BSs can be logically regarded as one virtual BS or a virtual set. Correspondingly, a BS usually serves multiple UEs, therefore, we denote the set $\mathcal{E}_m$ as the UEs to be served by BS $m \in \mathcal{M}$. In addition, the set $\mathcal{E}_m$ can be directly obtained when set $\mathcal{C}_k$ is given, where $k \in \mathcal{E}_m \Leftrightarrow m \in \mathcal{E}_k$. As shown in Fig. 1, unlike in the case of single link transmission, with multi-connectivity, the set ε_m generally overlaps with set $\mathcal{E}_{m'}$, for $m' \neq m$.

B. Signal Model for Collaborative Transmission

We consider a single carrier coherent transmission (i.e., multi-BS serves multi-UE over the same sub-carrier). For a typical UE, this will incur intra-BS interference from its serving BS and inter-BS interference from other BSs. We also consider the block fading channel model, where the channel remains unchanged during the coherent interval (i.e., coherent time and coherent frequency). Henceforth, the DL received signal of UE k can be formulated as

$$\begin{aligned} y_k &= \sum_{m\in\mathcal{C}_k} \mathbf{h}_{m,k}^{\dagger}\mathbf{w}_{m,k}x_k \\ &\quad + \sum_{k'\in\mathcal{K}_{-k}}\sum_{m'\in\mathcal{C}_{k'}} \mathbf{h}_{m',k}^{\dagger}\mathbf{w}_{m',k'}x_{k'} + z_k \\ &= \underbrace{\mathbf{H}_k^{\dagger}\mathbf{S}_k^{1/2}\mathbf{w}_k x_k}_{\text{multi-BS signal}} + \underbrace{\sum_{k'\in\mathcal{K}_{-k}} \mathbf{H}_k^{\dagger}\mathbf{S}_{k'}^{1/2}\mathbf{w}_{k'}x_{k'}}_{\text{multi-UE interference}} + \underbrace{z_k}_{\text{noise}}, \end{aligned} \quad (1)$$

where $\mathcal{K}_{-k} = \mathcal{K}\backslash k$ and x_k denotes the transmitted signals from BS $m \in \mathcal{E}_k$ to UE k with $\mathbb{E}\{|x_k|^2\} = 1$; $\mathbf{w}_{m,k} \in \mathbb{C}^{N\times 1}$ represents the DL beamforming vector from BS $m \in \mathcal{E}_k$ to UE k; $\mathbf{h}_{m,k} \in \mathbb{C}^{N\times 1}$ is the DL channel between BS $m \in \mathcal{C}_k$ and UE k; $z_k \sim \mathcal{CN}(0, \sigma^2)$ is the additive complex Gaussian noise (AWGN) with zero mean and variance σ^2 at UE k.

Denote the $(NM \times 1)$ complex concatenate vector $\mathbf{H}_k$ as the channels $\{\mathbf{h}_{m,k}, \forall m \in \mathcal{M}\}$ between the BS m and UE k. Likewise, we denote the concatenate vector $\mathbf{w}_k$ as the beamforming $\{\mathbf{w}_{m,k}, \forall m \in \mathcal{M}\}$. In addition, the concatenation of the beamforming vector $\{\mathbf{w}_{m,k'}, \forall m \in \mathcal{M}\}$ for UE k' is $\mathbf{w}_{k'}$. Besides, we define the block diagonal association matrix as $\mathbf{S} = (diag(\{s_{m,k}\}_{m\in\mathcal{M}}) \otimes \mathbf{I}_N) \in \mathbb{C}^{MN\times MN}$, where $s_{m,k}$ represents the integer scheduling variable of BS m to UE k. Specifically, $s_{m,k} = 1$ when UE k is scheduled by BS m, and $s_{m,k} = 0$ otherwise.

Given the received signal with the desired multi-BS coherent signal and multi-UE interference is represented in Eq. (1), the instantaneous received SINR of UE k can be represented as

$$\gamma_k = \frac{|\mathbf{H}_k^{\dagger}\mathbf{S}_k^{1/2}\mathbf{w}_k|^2}{\sum\limits_{k'\in\mathcal{K}_{-k}} |\mathbf{H}_k^{\dagger}\mathbf{S}_{k'}^{1/2}\mathbf{w}_{k'}|^2 + \sigma_z^2}, \quad (2)$$

where the SINR of UE k is jointly determined by the scheduling matrix $\mathbf{S}_k^{1/2}, \forall k \in \mathcal{K}$ and the beamforming $\mathbf{w}_k, \forall k \in \mathcal{K}$. Considering the overlapping and the multi-connectivity characteristics, the SINR of different UEs may influence each other when we independently optimize the scheduling variable.

C. Channel Estimation and Feedback

Noting that the transmit and receive antennas locate at different positions, CSI acquisition methods based on channel reciprocity or angular reciprocity can not be directly applied. Therefore, a conventional training-feedback-estimation procedure is considered in this paper. This procedure is available for both TDD and FDD modes, however, in this work, we focus on the FDD mode [23].

As illustrated in Fig. 1, the channel training and feedback process is executed between DBSs and CBSs, which are given the functions of data transmission and control channel transmission, respectively. This procedure is different from the conventional training-feedback process with two terminals (i.e., one UE and one BS). Channel information acquisition is more complicated since the DL pilot transmission, UE-side pilot feedback, and channel estimation are processed in different entities.[1] We consider a typical centralized function split[2] for more flexible coordinated transmission such that the beamforming and UL channel estimation is executed in the EC.

For the DL pilot transmission, we consider the orthogonal time-frequency pilot sequence allocation such that there is no pilot contamination for all UEs.

1) UL Feedback Channel: For simplicity, we exploit the traditional analog feedback, in which the unquantized QAM is leveraged [23]. Specifically, each UE feeds back the scaled pilots to the CBSs based on the DL received signal. The received DL pilot signal of UE k from BS m can be represented as

$$\mathbf{s}_{m,k} = \sqrt{\beta_1 P}\mathbf{h}_{m,k} + \mathbf{z}_{m,k}, \quad (3)$$

where BS m transmits the β_1 pilots to UE k with $\beta_1 \geq 1$. Here, the UL channel gain $\mathbf{g}_{m,k}^{\text{UL}}$ can be formulated as

$$\begin{aligned} \mathbf{g}_{m,k}^{\text{UL}} &= \frac{\sqrt{\beta_{\text{fb}}P}}{\sqrt{\beta_1 P + N_0}}\mathbf{s}_{m,k} + \widetilde{\mathbf{o}}_{m,k} \\ &= \frac{\sqrt{\beta_{\text{fb}}\beta_1}P}{\sqrt{\beta_1 P + N_0}}\mathbf{h}_{m,k} + \frac{\sqrt{\beta_{\text{fb}}\beta_1}P}{\sqrt{\beta_1 P + N_0}}\mathbf{z}_{m,k} + \widetilde{\mathbf{o}}_{m,k} \\ &= \frac{\sqrt{\beta_{\text{fb}}\beta_1}P}{\sqrt{\beta_1 P + N_0}}\mathbf{h}_{m,k} + \mathbf{o}_{m,k}. \end{aligned} \quad (4)$$

Note that both $\widetilde{\mathbf{o}}_{m,k}$ of the UL feedback and $\mathbf{z}_{m,k}$ of the DL-training phase are AWGN noise with the same noise variance N_0. P_{UL} is denoted as the per-symbol power over the UL feedback channel. Because $\widetilde{\mathbf{o}}_{m,k}$ and $\mathbf{z}_{m,k}$ are independently complex Gaussian distributed with the same variance $N_0\mathbf{I}$, the variance σ_o^2 of $\mathbf{o}_{m,k}$ denoted as a complex Gaussian can be calculated by

$$\sigma_o^2 = N_0\left(1 + \frac{\beta_{\text{fb}}P/N_0}{1 + \beta_1 P/N_0}\right), \quad (5)$$

where, for sake of simplicity, we assume the noise is the same for all UEs and BSs in both the UL and DL.

Note that we focus on the DL transmission, in this paper, we assume a simplified setting for the UL CSI feedback with an error-free unfaded AWGN channel with SNR $\frac{P_{\text{UL}}}{N_0}$, where P_{UL} is assumed to be the same for each UE in the UL channel feedback process.

[1] Actually, the dedicated training is needed for the coherent detection. Here, we focus on the DL association and coordinated beamforming, therefore, we neglect the additional round for the channel training.

[2] Like the centralized setting of cloud radio access network (C-RAN), we assume the full centralization in which Layer 1 to Layer 3 are fully implemented in the EC.

2) Training Channel With Feedback Error: The DL channel estimation is executed on the EC. Hence, on the basis of the UL channel $\mathbf{g}_{m,k}$, the channel can be estimated with MMSE estimator [35], where $\hat{\mathbf{h}}_{m,k}$ can be calculated by

$$\hat{\mathbf{h}}_{m,k} = \frac{\sqrt{\beta_{\text{fb}}\beta_1}P}{\sqrt{\beta_1 P + N_0}(\beta_{\text{fb}}P + N_0)}\mathbf{g}^{\text{UL}}_{m,k}. \tag{6}$$

When given the Eq.(4), the estimated channel $\widetilde{\mathbf{h}}_{m,k}$ in terms of the BS estimate in Eq.(6) and estimation error $\mathbf{e}_{m,k}$ can be denoted as

$$\widetilde{\mathbf{h}}_{m,k} = \hat{\mathbf{h}}_{m,k} + \mathbf{e}_{m,k}, \tag{7}$$

where $\mathbf{e}_{m,k}$ is the independent Gaussian noise with error variance σ_e^2 calculated by

$$\begin{aligned}\sigma_e^2 &= \frac{\sigma_w^2}{\sigma_w^2 + \frac{\beta_{\text{fb}}\beta_1 P^2}{\beta_1 P + N_0}} \\ &= \frac{1}{1+\beta_{fb}\frac{P}{N_0}} + \frac{\beta_{\text{fb}}\frac{P}{N_0}}{\left(1+\frac{P}{N_0}\right)\left(1+\beta_1\frac{P}{N_0}\right)}\end{aligned} \tag{8}$$

All of the DL training, pilots' feedback, CSI forwarding, and data transmission are implicitly assumed to perform in a frame with a long coherent sequence. In other words, the concatenation of the aforementioned process is smaller than the channel coherent time. However, it is also practical for the delay-feedback problems with the CSI changes frame by frame as the CSI is time-correlated [23]

IV. Problem Formulation

We aim at maximizing the weighted achievable sum rate under the constraints of maximum BS transmit power, UE/BS capacity limit, non-perfect channel conditions, and association schedules. Therefore, this optimization problem can be formulated as

$$\max_{\widetilde{\mathcal{W}},\mathbf{S}} \sum_{k\in\mathcal{K}} \delta_k \log(1+\gamma_k) \tag{9a}$$

$$\text{s.t. } 0 \le \sum_{k\in\mathcal{E}_m} \|\widetilde{\mathbf{w}}_{m,k}\|^2 \le p_{\max}, \quad \forall m \in \mathcal{M}, \tag{9b}$$

$$|\mathcal{E}_m| \le N, \quad \forall m \in \mathcal{M}, \tag{9c}$$

$$|\mathcal{E}_k| \le T, \quad \forall k \in \mathcal{K}, \tag{9d}$$

$$s_{m,k} \in \{0,1\}, \quad \forall m \in \mathcal{M}, \ \forall k \in \mathcal{K}, \tag{9e}$$

$$\gamma_k = \frac{\widetilde{\mathbf{w}}_k^{\dagger}\mathbf{S}_k^{1/2}\widetilde{\mathbf{H}}_k\widetilde{\mathbf{H}}_k^{\dagger}\mathbf{S}_k^{1/2}\widetilde{\mathbf{w}}_k}{\sum\limits_{k'\in\mathcal{K}_{-k}} \widetilde{\mathbf{w}}_{k'}^{\dagger}\mathbf{S}_{k'}^{1/2}\mathbf{H}_k\widetilde{\mathbf{H}}_k^{\dagger}\mathbf{S}_{k'}^{1/2}\widetilde{\mathbf{w}}_{k'} + \sigma_z^2},$$
$$\forall m \in \mathcal{M}, \quad \forall k \in \mathcal{K}, \tag{9f}$$

where the variable $\widetilde{\mathcal{W}} = \{\widetilde{\mathbf{w}}_1, \ldots, \widetilde{\mathbf{w}}_K\}$ denotes the set of beamforming in terms of non-perfect channel conditions. To provide fairness, we introduce the weight δ_k of each UE k. In problem (9a), we aim to maximize the total weighted network utility with optimal variable $\mathbf{S}^*$ and $\widetilde{\mathcal{W}}^*$. Constraint (9b) is the total power constraint for BS m which specifies that the sum of power consumption is no more than the power budget $p_{\max}$. Constraint (9c) indicates that each BS with N antennas serves at most N UEs. Constraint (9d) shows that the access-BS-num is limited to T. In addition, this assumption is reasonable not only because the number of UE antennas is limited, but also because a reasonable restriction on the access-BS-num can reduce the fronthaul load. Constraint (9e) is the binary scheduling variable between BS m and UE k. Constraint (9e) denotes the received SINR γ_k of UE k, and it is interfered by the beamformers from other UEs.

Considering the binary constraint (9c), (9d), (9e), and continuous constraint (9b), problem (9a) is a mixed-integer non-linear programming problem as there are variables in both of numerator and denominator of the received SINR. It is difficult to solve this NP-hard problem [33]. Therefore, we split it into a multi-connectivity scheduling and multi-UE power allocation sub-problem, respectively.

V. Swap-Based Many-to-Many Matching Algorithm

In this section, we first introduce the definition of many-to-many matching, and further propose the swap-matching for the many-to-many matching model. Then, we propose a swap-matching algorithm for the UE-BS multi-connectivity problem. The exchange stability and complexity of the algorithm are given.

A. Many-to-Many Matching

Inspired by the many-to-many matching theory, the UE-BS association is considered as a two-side matching with the set of UEs $\mathcal{K}$ and the set of BSs $\mathcal{M}$. Each UE or BS is denoted as a selfish player aiming to maximize its utility such that it can be formed as a matching game. With the help of a centralized control BS in FD-RAN, the information between two players can be fluently exchanged, and each payer has the global state information by communicating with the control BS. When UE_k is scheduled to BS_m, we say that UE_k and BS_m are pairwise matched. Thus, the two-side matching game between UEs $\mathcal{K}$ and BSs $\mathcal{M}$ can be formally defined as

Definition 1: The BS set $\mathcal{M} = 1, 2, \ldots, M$ and the UE set $\mathcal{K} = 1, 2, \ldots, K$ are defined as two disjoint sets for a many-to-many matching setting. $\mathcal{E}$ denotes the mapping between the UE set $\mathcal{K}$ and BS set $\mathcal{M}$, where a typical mapping pair of $BS_m \in \mathcal{M}$ and $UE_k \in \mathcal{K}$ is denoted as

1) $\mathcal{E}_m \subseteq \mathcal{K}$;
2) $\mathcal{E}_k \subseteq \mathcal{M}$;
3)$|\mathcal{E}_k| \le T$;
4) $|\mathcal{E}_m| \le N$;
5) $UE_k \in \mathcal{E}_m \Leftrightarrow BS_m \in \mathcal{E}_k$,

where the first condition implies that UEs matched with BS m belong to set $\mathcal{K}$, and BSs associated with UE k belong to the BS set $\mathcal{M}$ according to the second condition. In the third and fourth conditions, we define the maximum BS number N to access for one UE and the maximum UE number T to serve for one BS, respectively. This restriction is reasonable no matter from the perspective of capacity limit or the tolerable complexity. Because of the externalities or peer effects [36],

this formulated many-to-many game can not be simplified as a many-to-one game.

The externalities of the defined matching game come from the DL inter and intra-BS interference caused by co-channel communications [36]. Therefore, the association decisions are dynamically influenced by each other. The preference lists, a common definition for players, are introduced as an important reference to make association decisions. Here, the preference relation is denoted as $\succ$ for the players (i.e., UEs and BSs). For a typical $UE_k \in \mathcal{K}$, the preference list $\succ_{UE_k}$ over different $BS_m \in \mathcal{M}$, $BS_{m'} \in \mathcal{M}$ and $m \neq m'$ can be represented by

$$(BS_m, \Psi) \succ_{UE_k} (BS_{m'}, \Psi') \Leftrightarrow U_{m,k}(\Psi) > U_{m',k}(\Psi'), \quad (10)$$

where the notations Ψ and Ψ' denote the matchings $BS_m \in \Psi(UE_k)$ and $BS_{m'} \in \Psi'(UE_k)$, respectively. In Eq. (10), UE_k prefers BS_m rather than $BS_{m'}$ which is equal to the utility $U_{m,k}(\Psi)$ between matching Ψ is higher than utility $U_{m',k}(\Psi')$ between matching Ψ'. Likewise, for a typical $BS_m \in \mathcal{M}$, the preference list $\succ_{BS_m}$ over different $UE_k \in \mathcal{K}$, $UE_{k'} \in \mathcal{K}$ and $k \neq k'$ can be denoted as

$$(UE_k, \Psi) \succ_{BS_m} (UE_{k'}, \Psi') \Leftrightarrow U_{m,k}(\Psi) > U_{m,k'}(\Psi') \quad (11)$$

Different from the traditional two-sided matching [37], it is difficult to achieve stability even in a many-to-one matching [36]. Meanwhile, simple preference list-based acceptance criteria will not be directly applied in many-to-many matching with externalities. Therefore, to maximize the total utility in the network and achieve the stability of matching, we will introduce the concept of swap matching and design the swap-based many-to-many matching algorithm later.

B. Swap-Matching

In a traditional two-sided mapping setting (e.g., the house assignment problem), each UE chooses to accept or reject a mapping option [37], however, in the proposed swap-matching model, every two UEs try to exchange their associated BS index to improve the total utility while keeping the other associations unchanged.

To define the player's interdependency in terms of the peer effects more specifically when given the preference lists, we denote the swap blocking pair for every pared swap UEs as follows

Definition 2: Given two BS m and m', two UEs k and k', a matching Ψ with $BS_m \in \Psi(UE_k)$, $BS_{m'} \in \Psi(UE_{k'})$, and $BS_m \notin \Psi(UE_k)$, $BS_{m'} \notin \Psi(UE_m)$, a swap matching $\Psi^{km}_{k'm'} = \Psi \backslash \{(UE_k, BS_m), (UE_{k'}, BS_{m'})\} \cup \{(UE_k, BS_{m'}), (UE_{k'}, BS_m)\}$ is defined by the function $BS_{m'} \in \Psi^{km}_{k'm'}(UE_k)$, $BS_m \in \Psi^{km}_{k'm'}(UE_{k'})$ and $BS_{m'} \notin \Psi^{km}_{k'm'}(UE_{k'})$, $BS_m \notin \Psi^{km}_{k'm'}(UE_k)$.

Specifically, the swap-matching for UE k and k' refers to an exchange that occurred between their associated BS with keeping UE $k \in \mathcal{K}_{\backslash\{k,k'\}}$ remaining unchanged. With the centralized FD-RAN architecture, the flexible information exchange between every paired player is reasonable and practical which has been particularly noteworthy.

However, a reasonable swap operation generation requires a sufficient driving force, that is, the utility of the two after the exchange is greater than that before the swap-matching. Therefore, to better define the conditions under which the swap operation occurs, we introduce the definition of swap-blocking pairs, as shown below

Definition 3: Given a matching Ψ and a pair $(UE_k, UE_{k'})$ with UE_k and $UE_{k'}$ matched in Ψ, if there exist $BS_m \in \Psi(UE_k)$ and $BS_{m'} \in \Psi(UE_{k'})$ such that

1)$\forall t \in \{UE_k, UE_{k'}, BS_m, BS_{m'}\}, (\Psi^{km}_{k'm'}(t), \Psi^{km}_{k'm'}) \succeq_t (\Psi(t), \Psi)$,

2)$\exists t \in \{UE_k, UE_{k'}, BS_m, BS_{m'}\}, (\Psi^{km}_{k'm'}(t), \Psi^{km}_{k'm'}) \succ_t (\Psi(t), \Psi)$, then swap matching $\Psi^{km}_{k'm'}$ is approved, and $(UE_k, UE_{k'})$ is called a swap-blocking pair in Ψ.

According to the above definition, the condition of a swap operation is that the utility of all players after the exchange will not decrease, and the utility of at least one UE will be improved.

We can define the matching behaviors between UE and BS based on the above definitions. Every two UEs first transmit the potential swappable BS index to the EC via the independent control channels with control BSs. After that, the EC will exchange the connected BS index of these two UEs and compute the post-swap total utility. At last, the swap operation will be confirmed under the circumstances that the total utility can get improved. Through several swap operations, the BS index of each UE can reach a stable matching, which is also denoted as a two-sided exchange stable matching.

C. UE-BS Swap-Matching Algorithm

With the definition of swap-matching, we propose a many-to-many matching algorithm called UE-BS swap-matching algorithm (UBSA), aiming at finding a stable matching for UE-BS multi-connectivity. There are two phases in the proposed algorithm, that is the *Initialize phase* and *Swap-matching phase*.

In the *Initialize phase*, it is necessary to initialize the association matrix $\mathcal{A}$ as a zero matrix and the index set $\mathbb{I}_k$ as an empty set of each UE for the UE-BS association and associated BS index storage, respectively. Besides, the connections are established according to the DL RSRP $\mathcal{R}$. The algorithm (1) starts with the iterative selection of each UE to access the BS with the largest RSRP, i.e., $m^* = \arg\max_{m \in \mathcal{M}} \mathcal{R}_k$. However, it should be noted that the number of UEs served by each BS cannot exceed the maximum served num N. If the BS which UE k tries to access with index m^* is fully loaded, the UE k should select another BS with the largest RSRP except for the BS m^*, until a BS that meets the load requirements is found. After that, for each UE k, the sub-optimal BS with index m^* will be added to the set $\mathbb{I}_k$.

In the *Swap-matching phase*, two different UEs try to exchange their associated BSs under the condition that the total utility $U^{\text{total}} = \sum_{k=1} \delta_k \log(1 + \gamma_k)$ denoted as the sum achievable capacity gets improved. For instance, first of all, UE k and k' exchange one of their associated BS index. After that, the total utility $U^{\text{total}}_{\text{after}}$ in terms of the

post-exchange associations is calculated. At last, if no total utility improvement after the swap operation, this exchange is not confirmed, otherwise save the exchanged BS index. The detailed UBSA description which includes the initialization part and the swap-matching part is described in Algorithm (1).

It's worth noting that the swap-based association has a different time scale compared with the beamforming procedure. Like the general time scales of handover versus resource allocation in LTE or NR systems, multiple mini-slots exist for beamforming during a predefined association time period. This swap operation can be determined in the EC without signaling exchange between control BS and UEs. Besides, we can calculate the association in Algorithm (1) according to the channel information from the first mini time slot, and subsequently, reduce the control signaling overhead.

Algorithm 1 UE-BS Swap-Matching Algorithm (UBSA)

Initialize phase
Initialize the association matrix $\mathcal{A}, \forall \mathcal{A}_{k,m} = 0$;
Initialize the index set $\mathbb{I}_k = \varnothing$;
Initialize DL RSRP matrix $\mathcal{R}$;
for *each UE* $k \in \mathcal{K}$ **do**
  Initialize the iteration index $i = 0$;
  if $i \leq N$ **then**
    Choose $m^* = \arg\max_{m \in \mathcal{M}} \mathcal{R}_k$
    while $|\mathcal{A}_{m^*}| \leq N$ **do**
      Remove the RSRP value, i.e., $\mathcal{R}_{k,m^*} = 0$;
      $m^* = \arg\max_{m \in \mathcal{M}} \mathcal{R}_k$;
    Save the BS index $\mathbb{I}_k = \mathbb{I}_k \cup m^*$
    Set the association $\mathcal{A}_{k,m^*} = 1$;
    $i = i + 1$;
Swap-matching phase
for *UE* $k = 1, \cdots, K$ **do**
  for *UE* $k' = k+1, \cdots, K$ **do**
    for *BS* i *in* $\mathbb{I}_k$ **do**
      for *BS* j *in* $\mathbb{I}_{k'}$ **do**
        Calculate the total utility $U^{\text{total}}(\Psi)$before swap operation;
        Delete the association $\mathcal{A}_{k,i} = 0$ and $\mathcal{A}_{k',j} = 0$;
        Add the association $\mathcal{A}_{k,j} = 1$ and $\mathcal{A}_{k',i} = 1$;
        Calculate the total utility $U^{\text{total}}(\Psi^{k,i}_{k',j})$ after swap operation;
        if $U^{total}(\Psi^{k,i}_{k',j}) \leq U^{total}(\Psi)$ **then**
          Recover the association $\mathcal{A}_{k,i} = 1$;
          Recover the association $\mathcal{A}_{k',j} = 1$;
Save the association matrix $\mathcal{A}$.

D. Effectiveness, Stability, and Complexity

1) Effectiveness: According to Algorithm (1), for UE k and k' with associated BS i and j, respectively, the swap operation occurs under the condition that the total utility after the swap operation is higher than that before, i.e., $U^{\text{total}}(\Psi^{k,i}_{k',j}) > U^{\text{total}}(\Psi)$, and it can be detailed represented as

$$\begin{aligned}\Phi_{\Psi \to \Psi^{k,i}_{k',j}} &= U^{\text{total}}(\Psi^{k,i}_{k',j}) - U^{\text{total}}(\Psi) \\ &= \Big(\big(\delta_k \log(1+\gamma_k), \Psi^{k,i}_{k',j}\big) \\ &\quad - \big(\delta_k \log(1+\gamma_k), \Psi\big) \Big) > 0. \end{aligned} \tag{12}$$

Hence, $\Phi_{\Psi \to \Psi^{k,i}_{k',j}}$ denoted as the utility difference is always positive, which means that the proposed USBA is effective.

2) Stability: If a two-side matching with iterative swap operation converges to a stable matching Ψ^*, Ψ^* is a swap-matching with stability.

Proof: According to definition 3, if a typical swap blocking pair (UE_i, UE_j) with $\{UE_i, UE_{j'}, BS_k, BS_{k'}\}$, $\forall t, U^{total}(\Psi^{ik}_{j'k'}(t), \Psi^{ik}_{j'k'}) \succeq_t U^{total}(\Psi(t), \Psi^*)$, and $\exists t \in \{UE_i, UE_{j'}, BS_k, BS_{k'}\}$, $U^{total}(\Psi^{ik}_{j'k'}(t), \Psi^{ik}_{j'k'}) \succ_t U^{total}(\Psi(t), \Psi^*)$ still exists in the final matching Ψ^*, UBSA will not terminate until this swap-blocking pair is removed, which in turn conflicts with the denoted stable matching Ψ^*. Hence, the convergence to a stable swap-matching at the end of the algorithm is proved. ■

3) Cmplexity: The complexity of the UBSA algorithm can be analyzed separately in two phases. For the initialize phase, the inner loop for sorting the RSRP is converged with the complexity $O(M^2)$. Considering the first and second loops with complexity $O(K)$ and $O(N)$, respectively, the total complexity of the initialize phase is $O(KNM^2)$. For the swap-matching phase, the cardinality of the set $\mathbb{I}_k$ and $\mathbb{I}_{k'}$ are both T when each UE is fully matched. Since the computation complexity of U^{total} is $O(1)$, the total complexity of the swap-matching phase is $O(K^2T^2)$. It is can be seen that the computation complexity of either the initialize or swap-matching phase is lower than that of exhaustive search with an exponentially increasing complexity.

VI. Coordinated Multi-Connectivity Beamforming Algorithm

In this section, a coordinated beamforming problem is defined, provided that the UE-BS associations are pre-calculated by the Algorithm (1). Besides, because of the non-convex objective function, a simplified version in terms of second-order relaxation is proposed.

A. Problem Analysis and Power Allocation

Noting that the UE-BS associations are given, the simplified joint beamforming problem can be formulated as

$$\begin{aligned} \max_{\widetilde{\mathcal{W}}} \quad & \sum_{k \in \mathcal{K}} \delta_k \log(1+\gamma_k) \\ \text{s.t.} \quad & (9b), (9f). \end{aligned} \tag{13a}$$

Based on the objective function in problem (13) and the equality constraints in (9f), we can formulate the Lagrangian

function with multiplier vector $\mathbf{v} = [v_1, \ldots, v_K]$ as

$$\mathcal{L}(\widetilde{\mathcal{W}}, \boldsymbol{\gamma}, \mathbf{v}) = \sum_{k\in\mathcal{K}} \delta_k \log(1+\gamma_k) - \sum_{k\in\mathcal{K}} v_k \big(\gamma_k - \frac{\widetilde{\mathbf{w}}_k^{\dagger}\mathbf{S}_k^{1/2}\widetilde{\mathbf{H}}_k\mathbf{H}_k^{\dagger}\mathbf{S}_k^{1/2}\widetilde{\mathbf{w}}_k}{\sum\limits_{k'\in\mathcal{K}_{-k}} \widetilde{\mathbf{w}}_{k'}^{\dagger}\mathbf{S}_{k'}^{1/2}\widetilde{\mathbf{H}}_{k'}\widetilde{\mathbf{H}}_{k'}^{\dagger}\mathbf{S}_{k'}^{1/2}\widetilde{\mathbf{w}}_{k'} + \sigma_z^2}\big), \tag{14}$$

where $\boldsymbol{\gamma} = \{\gamma_1, \ldots, \gamma_K\}$ denotes the SINR vector. When fixing the beamforming $\widetilde{\mathcal{W}}$, the Lagrange multiplier v_k can be derived by differentiating the variables γ_k in formula (14), which can be denoted as

$$v_k = \delta_k \frac{\left(\sum\limits_{k'\in\mathcal{K}_{-k}} \widetilde{\mathbf{w}}_{k'}^{\dagger}\mathbf{S}_{k'}^{1/2}\mathbf{H}_{k'}\widetilde{\mathbf{H}}_{k'}^{\dagger}\mathbf{S}_{k'}^{1/2}\widetilde{\mathbf{w}}_{k'} + \sigma_z^2\right)}{\sum\limits_{k'\in\mathcal{K}} \widetilde{\mathbf{w}}_{k'}^{\dagger}\mathbf{S}_{k'}^{1/2}\widetilde{\mathbf{H}}_{k'}\widetilde{\mathbf{H}}_{k'}^{\dagger}\mathbf{S}_{k'}^{1/2}\widetilde{\mathbf{w}}_{k'} + \sigma_z^2} \tag{15}$$

Given the Eq. (15), the Lagrange function in (14) can be reformulated as

$$f_0(\widetilde{\mathcal{W}}, \boldsymbol{\gamma}) = \sum_{k\in\mathcal{K}} \delta_k \log(1+\gamma_k) - \sum_{k\in\mathcal{K}} \delta_k\gamma_k + \sum_{k\in\mathcal{K}} \frac{\delta_k(1+\gamma_k)\widetilde{\mathbf{w}}_k^{\dagger}\mathbf{S}_k^{1/2}\widetilde{\mathbf{H}}_k\widetilde{\mathbf{H}}_k^{\dagger}\mathbf{S}_k^{1/2}\widetilde{\mathbf{w}}_k}{\sum\limits_{k'\in\mathcal{K}} \widetilde{\mathbf{w}}_{k'}^{\dagger}\mathbf{S}_{k'}^{1/2}\mathbf{H}_{k'}\widetilde{\mathbf{H}}_{k'}^{\dagger}\mathbf{S}_{k'}^{1/2}\widetilde{\mathbf{w}}_{k'} + \sigma_z^2}, \tag{16}$$

Herein, the optimization (13) can be reformulated as

$$\begin{aligned} &\max_{\widetilde{\mathcal{W}},\boldsymbol{\gamma}} \quad f_0(\widetilde{\mathcal{W}}, \boldsymbol{\gamma}) \\ &\text{s.t. } (9b), (9f). \end{aligned} \tag{17a}$$

Proposition 1: The optimization problem (17) can be decomposed as an outer sub-problem over variable $\mathcal{W}$ and inner sub-problem over variable $\boldsymbol{\gamma}$, respectively.

Proof: When given the beamforming $\widetilde{\mathcal{W}}$, the inner problem can be represented as

$$\begin{aligned} &\max_{\gamma} \quad \sum_{k\in\mathcal{K}} \delta_k \log(1+\gamma_k) \\ &\text{s.t. } (9f). \end{aligned} \tag{18a}$$

The inequality in (9f) holds, provided that the inner problem is convex over variable $\boldsymbol{\gamma}$. According to the strong duality condition, the inner optimization problem is equivalent to the dual problem, which can be represented by

$$\underset{\mathbf{v}\succeq 0}{\text{minimize}} \quad \underset{\boldsymbol{\gamma}}{\text{maximize}} \quad f_0(\widetilde{\mathcal{W}}, \boldsymbol{\gamma}, \mathbf{v}) \tag{19}$$

The optimal value $(\boldsymbol{\gamma}^*, \mathbf{v}^*)$ can be derived by the first order condition $\partial\mathcal{L}(\widetilde{\mathcal{W}}, \boldsymbol{\gamma}, \mathbf{v})/\partial\gamma_k$. Herein, the optimal multiplier v_k^* can be represented by

$$v_k^* = \frac{\delta_k}{1+\gamma_k^*}, \tag{20}$$

which has also been represented in Eq. (15). Since the optimal Lagrange multiplier $v_k^* \geq 0$, the inner optimization problem can be further represented as

$$\underset{\boldsymbol{\gamma}}{\text{maximize}} \quad f_0(\widetilde{\mathcal{W}}, \boldsymbol{\gamma}, \mathbf{v}^*) \tag{21}$$

Therefore, the problem (17) is equivalent to (13). ■

Note that problem (17) is still non-convex because the optimization variables can be found in both numerator and nominator. By exploiting second-order relaxation from the FP in [30], the objective function of (17) can be reformulated as

$$\begin{aligned} f_1(\widetilde{\mathcal{W}}, \boldsymbol{\gamma}, \boldsymbol{\beta}) &= \sum_{k\in\mathcal{K}} \delta_k \left(\log(1+\gamma_k) - \gamma_k\right) \\ &+ \sum_{k\in\mathcal{K}} \left(2\sqrt{\delta_k(1+\gamma_k)}\mathrm{Re}\left\{\beta_k^*\widetilde{\mathbf{w}}_k^{\dagger}\mathbf{S}_k^{1/2}\widetilde{\mathbf{H}}_k\right\}\right. \\ &\left. - |\beta_k|^2\left(\sum_{k'\in\mathcal{K}} \widetilde{\mathbf{w}}_{k'}^{\dagger}\mathbf{S}_{k'}^{1/2}\widetilde{\mathbf{H}}_{k'}\widetilde{\mathbf{H}}_{k'}^{\dagger}\mathbf{S}_{k'}^{1/2}\widetilde{\mathbf{w}}_{k'} + \sigma_z^2\right)\right), \end{aligned} \tag{22}$$

where the vector $\boldsymbol{\beta} = [\beta_1, \ldots, \beta_K]$ is introduced as a new auxiliary variable required by fractional programming, and $Re\{\cdot\}$ denotes the real part of a complex number. Eq. (22) has a summation form making it easier to solve than that in Eq. (14). Besides, $f_1(\widetilde{\mathcal{W}}, \boldsymbol{\gamma}, \boldsymbol{\beta})$ in (22) is concave over variable β. Note that Eq. (14) can be derived from (22) by partial derivative of (22) with respect to $\boldsymbol{\beta}$, i.e., $f_0(\widetilde{\mathcal{W}}, \boldsymbol{\gamma}, \mathbf{v}) = \underset{\boldsymbol{\beta}}{\text{maximize}} \ f_1(\widetilde{\mathcal{W}}, \boldsymbol{\gamma}, \beta)$.

Proposition 2: The following problem

$$\begin{aligned} &\max_{\widetilde{\mathcal{W}},\boldsymbol{\gamma},\boldsymbol{\beta}} \quad f_1(\widetilde{\mathcal{W}}, \boldsymbol{\gamma}, \boldsymbol{\beta}) \\ &\text{s.t. } (9b), \end{aligned} \tag{23a}$$

is a typical quadratically constrained quadratic program (QCQP) problem over variable $\widetilde{\mathcal{W}}$ on the condition that both the variable $\boldsymbol{\gamma}$ and $\boldsymbol{\beta}$ are fixed.

According to the proposition (2), here, by taking the partial derivative $\partial f_1(\widetilde{\mathcal{W}}, \boldsymbol{\gamma}, \boldsymbol{\beta})/\partial\boldsymbol{\beta}$ to zero, the optimal β_k^* can be calculated by

$$\beta_k{}^* = \frac{\sqrt{\delta_k(1+\gamma_k)}\widetilde{\mathbf{w}}_k^{\dagger}\mathbf{S}_k^{1/2}\widetilde{\mathbf{H}}_k}{\sum\limits_{k'\in\mathcal{K}} \widetilde{\mathbf{w}}_{k'}^{\dagger}\mathbf{S}_{k'}^{1/2}\widetilde{\mathbf{H}}_{k'}\mathbf{H}_{k'}^{\dagger}\mathbf{S}_{k'}^{1/2}\widetilde{\mathbf{w}}_{k'} + \sigma_z^2}. \tag{24}$$

To further simplify problem. (23), which is non-convex, we define the following function as

$$f_2(\widetilde{\mathcal{W}}, \boldsymbol{\gamma}, \boldsymbol{\beta}, \boldsymbol{\mu}) = f_1(\widetilde{\mathcal{W}}, \boldsymbol{\gamma}, \boldsymbol{\beta}) - \sum_{m\in\mathcal{M}} \mu_m \left(\sum_{k\in\mathcal{E}_m} \|\widetilde{\mathbf{w}}_{m,k}\|_2^2 - p_{\max}\right), \tag{25}$$

where $\boldsymbol{\mu} = [\mu_1, \ldots, \mu_m]$ are the Lagrange multipliers corresponding to constraint (9b). Therefore, (23) can be

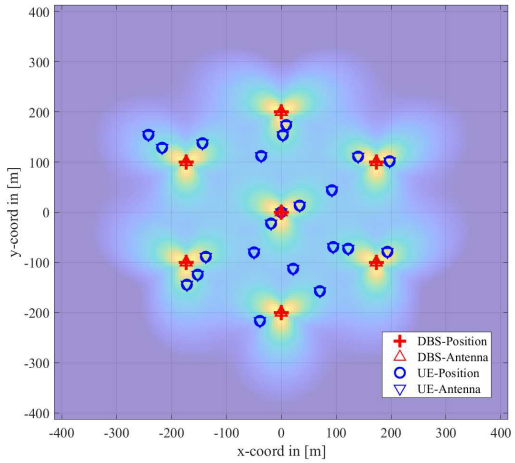

Fig. 2. The simulation scenario based on 3GPP 36.873 UMI channel model (light load).

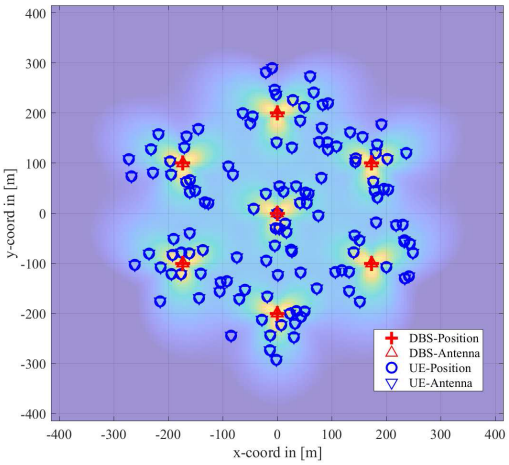

Fig. 3. The simulation scenario based on 3GPP 36.873 UMI channel model (heavy load).

reformulated as

$$\max_{\boldsymbol{\gamma},\widetilde{\mathcal{W}},\boldsymbol{\beta},\boldsymbol{\mu}} \quad f_2(\widetilde{\mathcal{W}},\boldsymbol{\gamma},\boldsymbol{\beta},\boldsymbol{\mu}) \quad \text{s.t. } (9f) \tag{26a}$$

Problem (26) is an unconstrained optimization problem when $\boldsymbol{\gamma}$ and $\boldsymbol{\beta}$ are fixed in Eq. (9f) and (24), respectively. By taking the partial derivative $\partial f_2(\widetilde{\mathcal{W}},\boldsymbol{\gamma},\boldsymbol{\beta},\boldsymbol{\mu})/\partial\widetilde{\mathbf{w}}_k$ to zero, the optimal beamforming can be calculated by

$$\widetilde{\mathbf{w}}_k = \sqrt{\delta_k(1+\gamma_k)}\beta_k^* \times \left(\sum_{k'\in\mathcal{K}} |\beta_{k'}|^2 \mathbf{S}_{k'}^{1/2}\widetilde{\mathbf{H}}_{k'}\widetilde{\mathbf{H}}_{k'}^{\dagger}\mathbf{S}_{k'}^{1/2} + \mathbf{D}_k\right)^{-1} \mathbf{S}_k^{1/2}\widetilde{\mathbf{H}}_k \tag{27}$$

where $\mathbf{D}_k = (\text{diag}(\{\mu_m\}_{m\in\mathcal{C}_k}) \otimes \mathbf{I}_N)$. This optimal $\widetilde{\mathbf{w}}_k$ is similar to a minimum mean-square-error beamformer [29].

B. Beamforming Algorithm Design

We propose a multi-BS multi-UE coordinated beamforming (MBMCB) (2). In Algorithm (2), the beam generation is based on the alternating optimization, also known as the block coordinate descent algorithm. At the beginning of the algorithm, it is necessary to calculate an initial input, therefore, conjugate beamforming also called maximum ratio transmission (MRT) beamforming is leveraged to initialize this algorithm, which can be denoted as

$$\widetilde{\mathbf{w}}_{m,k} = \sqrt{\frac{p}{|\mathcal{E}_m|}}\frac{\widetilde{\mathbf{h}}_{m,k}}{\|h_{m,k}\|}. \tag{28}$$

In the proposed algorithm, the variables $\boldsymbol{\gamma}$, $\boldsymbol{\beta}$ and $\mathcal{W}$ are iteratively optimized. It is worth noting that in the 7-th step, changing μ_m will not have a significant impact on the beamforming of other BSs, therefore, we can simplify the solution of the problem by independently calculating the Lagrangian multipliers of each base station [33].

Cmplexity: The complexity for initializing the beamformer $\widetilde{\mathbf{w}}_{m,k}$ is $O(MK)$. The alternating optimization started from the 5-th step, and hence we only consider the complexity of the inner loop. To calculate the optimal beamformer for each BS, we exploit the bisection search method. The main complexity comes from the pseudo-inverse of the matrix in Eq.(27). Besides, because the complexity of

Algorithm 2 Multi-BS Multi-UE Coordinated Beamforming (MBMCB)

```
Input parameters: S, K, M;
for each UE k ∈ K do
    for each BS m ∈ M do
        Initialize the beamformer for each UE w̃_{m,k} from Eq. (28);
while not converge do
    for each UE k ∈ K do
        Calculating γ according to (9e);
    for each UE k ∈ K do
        Calculating β according to (24);
    for each BS m ∈ M do
        Initialize the BS power budget f_min, f_mid and f_max;
        Initialize the bisection parameter μ_min and μ_max;
        Initialize the iteration parameter n_iter = 0, and
        maximum iteration steps n_max;
        while f_max − f_min > ϵ and n_iter = 0 < n_max do
            for each UE k ∈ K and do
                if s_{k,m} = 1 then
                    Calculating f_min with μ_min;
                    Calculating f_mid with (μ_min + μ_max)/2;
                    Calculating f_max with μ_max;
            if f_mid > p_max then
                μ_min ← (μ_min + μ_max)/2;
            else
                μ_max ← (μ_min + μ_max)/2;
            n_iter = n_iter + 1;
    Output the beamfoming w̃_k of each UE k.
```

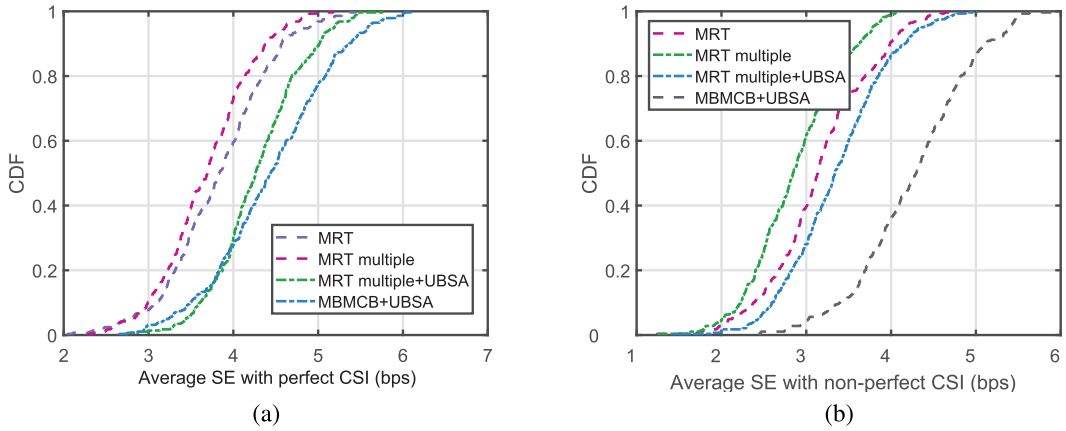

Fig. 4. CDF of average SE a) perfect CSI. b) non-perfect CSI.

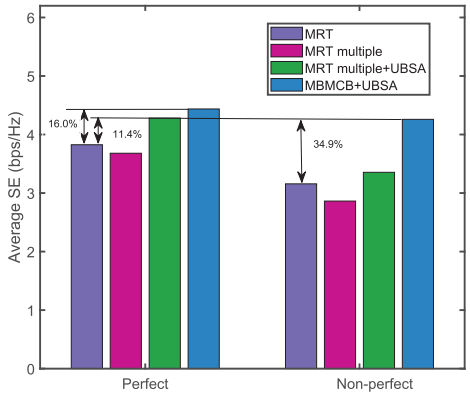

Fig. 5. Average SE versus different channel conditions.

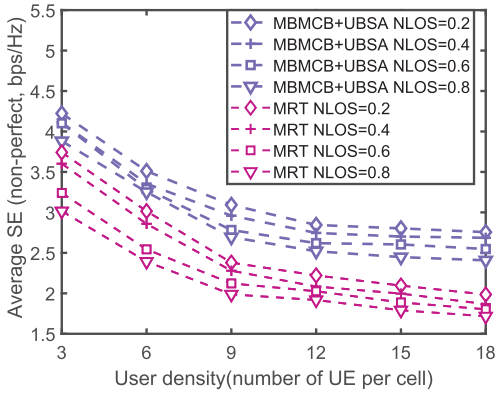

Fig. 6. Average SE versus different NLOS ratios.

Eq.(27) is $O((KNM)^3)$, the total complexity of the bisection search is $O(Mn_{max}(KNM)^3)$, where n_{max} is denoted as the maximum iteration steps. Therefore, the total complexity of Algorithm (2) is $O(Mn_{max}(KNM)^3)$.

VII. Simulation Results

As shown in Fig. 2 and Fig. 3, we consider 7-hexagon urban micro cells, each having a radius of 200m. Each cell consists of three sectors(i.e., three BSs), and is equipped with a linear antenna array with $N = 10$ antennas. As illustrated in Fig. 2, we consider a basic setting that there are three UEs generated independently in each cell. A circular exclusion region with a radius of 20m is considered. We set the maximum DL transmit power as 43 dBm. The thermal noise figure of each UE is set to -114 dBm. The communication bandwidth is set to unit 1. We restrict the maximum number of BSs that a UE can be connected to is set as 3. The importance weights δ_k for the proportional fairness are set as 1 for each UE. In addition, the DL channel is generated according to the standard 3GPP 36.873 urban micro (UMI) channel in terms of the QuaDRiGa simulation environment [38].

In the simulation part, we focus on the performance of four algorithms which can be listed below:

- **MRT**: MRT beamforming formulated in Eq. (28) is a traditional linear beamforming method with low complexity. Here, we take the single-connectivity MRT which is referred to as MRT (i.e. each UE access to only one BS) as a baseline algorithm.
- **MRT Multiple**: This algorithm considers the MRT beamforming in terms of the multi-connectivity. Besides, this multi-connectivity is simply depending on the DL RSRP.
- **MRT Multiple+UBSA**: As illustrated on Alg. (1), this algorithm adds a swap-matching procedure on the basis of multi-connectivity compared to **MRT Multiple** algorithms.
- **MBMCB+UBSA**: This algorithm is a combination of two proposed algorithms (i.e., the coordinated beamforming algorithm on Alg. (2) and the swap-matching algorithm on Alg. (1)).

A. Average Spectral Efficiency Versus Different Algorithms

In Fig. 4a, as illustrated in the cumulative distribution function (CDF) of average spectrum efficiency (SE) with perfect CSI, MAMCB+UBSA has the higher average SE in contrast to other algorithms. It is worth noting that, MRT Multiple performs worse on average SE than MRT single-connectivity. This is because the power is equally allocated to each association which in turn causes severe interference. In addition, we can see that the MBMCB +UBSA and MRT+UBSA can achieve nearly the same average SE at

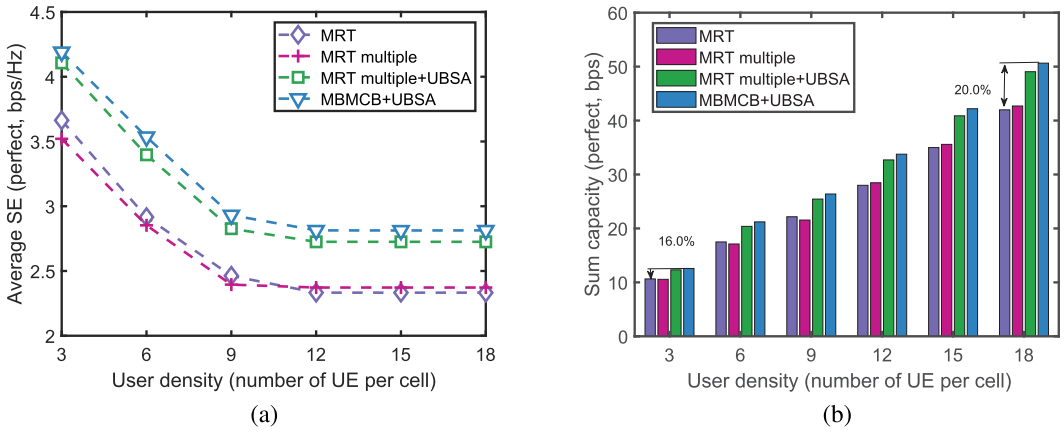

Fig. 7. The average SE a) and sum capacity b) with perfect CSI.

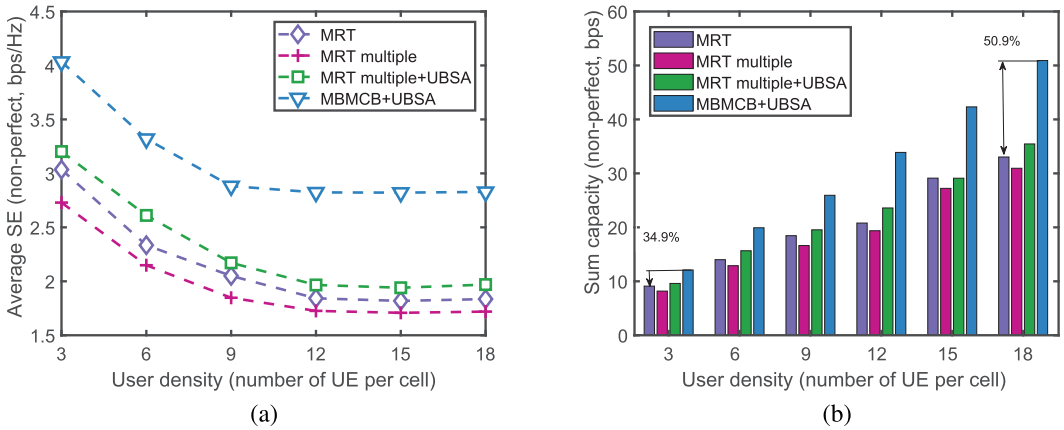

Fig. 8. The average SE a) and sum capacity b) with non-perfect CSI.

the low SE stage, which shows the superiority of the UBSA algorithm.

In Fig. 4b, we further investigate the CDF of non-perfect CSI versus different algorithms. Both Fig.4a and Fig. 4b show that, simple multi-connectivity without any association scheduling and power optimization can not bring SE gain. Furthermore, compared to Fig.4, MRT+UBSA can get little SE improvement. The biggest difference from the perfect CSI condition in Fig. 4 is that MAMCB+UBSA can increase the average SE. This result shows the effectiveness of the proposed MAMCB beamforming algorithm.

Fig. 5 shows the sum capacity versus different algorithms under perfect and non-perfect CSI conditions. MBMCB+UBSA has 16.0% average SE improvement under perfect channel conditions, while it can achieve 34.9% average SE improvement under non-perfect channel conditions. We observe that, even with the non-perfect CSI, MBMCB+UBSA has nearly 11.4% average SE when in contrast to it with perfect CSI.

B. Average Spectral Efficiency Versus Different NLOS Ratios

As illustrated in Fig. 6, we study the impact of different non-line-of-sight (NLOS) ratios (i.e. the ratio of the number of non-line-of-sight UEs to the total number of UEs) on the system throughput. Meanwhile, we choose two representative algorithms (i.e. MBMCB+UBSA and MRT). We can find that the system throughput decreases with the NLOS ratio increasing under both the perfect and non-perfect conditions. This is reasonable as the beamforming performance will be significantly degraded under NLOS channel conditions. When the UE density increases, the average SE decreases quickly. However, we can find that MBMCB+UBSA has less performance degradation compared with MRT.

C. Average Spectral Efficiency Versus Different UE Densities

Fig. 7a and Fig. 8a show the influence of different UE densities on average SE and total throughput. It can be seen in Fig. 8a that, with the number of UE per cell increases, the average SE first decreases quickly, then becomes constant. In addition, the average SE by MRT Multiple gradually exceeds that by MRT when UE density increases. This indicates that under perfect channel conditions, UEs become denser. This to some extent shows that under perfect channel conditions, as UEs become denser, using multiple connections seems to be a better solution in terms of improving SE than a single connection. From another aspect, we can see that under perfect channel conditions, exploiting the Multiple+UBSA algorithm can achieve good performance improvements with different UE densities. As shown in Fig. 8a, except for the MBMCB+UBSA, the average SE of other proposed algorithms still slowly decreases as the UE density continuously increases. Therefore, we can see

that the proposed MBMCB+UBSA has strong robustness in terms of different user densities. Different from the excellent performance of the MRT multiple+UBSA under perfect channel conditions, the average SE improvement brought by it is not very obvious under imperfect channel conditions.

Furthermore, we can see from Fig. 7b and Fig. 8b that the overall throughput improvement (i.e., from 34.9% to 50.9%) of MBMCB+UBSA with non-perfect CSI when compared with that (i.e., from $16.\%$ to 20.0%) with perfect CSI.

VIII. Conclusion

In this paper, we have proposed a flexible downlink multi-connectivity and dynamic resource cooperation framework in downlink fully-decoupled radio access networks. We have introduced a two-stage channel estimation scheme in the downlink FD-RAN. We have decomposed the problem into a multi-connectivity sub-problem and a beamforming sub-problem, which were solved by a swap-based many-to-many matching algorithm and a fractional programming algorithm, respectively. The simulation results based on standard 3GPP 36.873 urban micro channel have shown the superiority of our proposed algorithms. In the future, we will further design efficient network control and dynamic management approach with limited network status feedback for the introduced FD-RAN architecture.

References

[1] W. Saad, M. Bennis, and M. Chen, "A vision of 6G wireless systems: Applications, trends, technologies, and open research problems," *IEEE Netw.*, vol. 34, no. 3, pp. 134–142, Oct. 2020.

[2] H. Zhou, W. Xu, J. Chen, and W. Wang, "Evolutionary V2X technologies toward the Internet of Vehicles: Challenges and opportunities," *Proc. IEEE*, vol. 108, no. 2, pp. 308–323, Feb. 2020.

[3] B. Mao, Y. Kawamoto, and N. Kato, "AI-based joint optimization of QoS and security for 6G energy harvesting Internet of Things," *IEEE Internet Things J.*, vol. 7, no. 8, pp. 7032–7042, Aug. 2020.

[4] J. Kang et al., "Communication-efficient and cross-chain empowered federated learning for artificial intelligence of things," *IEEE Trans. Netw. Sci. Eng.*, vol. 9, no. 5, pp. 2966–2977, Sep. 2022.

[5] B. Qian, H. Zhou, T. Ma, K. Yu, Q. Yu, and X. Shen, "Multi-operator spectrum sharing for massive IoT coexisting in 5G/B5G wireless networks," *IEEE J. Sel. Areas Commun.*, vol. 39, no. 3, pp. 881–895, Mar. 2020.

[6] F. Tang, Y. Zhou, and N. Kato, "Deep reinforcement learning for dynamic uplink/downlink resource allocation in high mobility 5G HetNet," *IEEE J. Sel. Areas Commun.*, vol. 38, no. 12, pp. 2773–2782, Dec. 2020.

[7] Q. Yu et al., "A fully-decoupled RAN architecture for 6G inspired by neurotransmission," *J. Commun. Inf. Netw.*, vol. 4, no. 4, pp. 15–23, Dec. 2019.

[8] R. Ebrahimi, H. Zamiri-Jafarian, and M. Khademi, "A smart pilot assignment in multi-cell massive MIMO systems using virtual modeling of assigning cost," *IEEE Trans. Signal Process.*, vol. 69, pp. 2468–2480, 2021.

[9] X. Wang et al., "Energy-efficient virtual base station formation in optical-access-enabled cloud-RAN," *IEEE J. Sel. Areas Commun.*, vol. 34, no. 5, pp. 1130–1139, May 2016.

[10] M. Guo and M. C. Gursoy, "Joint activity detection and channel estimation in cell-free massive MIMO networks with massive connectivity," *IEEE Trans. Commun.*, vol. 70, no. 1, pp. 317–331, Jan. 2022.

[11] H. Du, J. Kang, D. Niyato, J. Zhang, and D. I. Kim, "Reconfigurable intelligent surface-aided joint radar and covert communications: Fundamentals, optimization, and challenges," *IEEE Veh. Technol. Mag.*, vol. 17, no. 3, pp. 54–64, Sep. 2022.

[12] W. Sun, L. Wang, J. Liu, N. Kato, and Y. Zhang, "Movement aware CoMP handover in heterogeneous ultra-dense networks," *IEEE Trans. Commun.*, vol. 69, no. 1, pp. 340–352, Jan. 2021.

[13] Y. Gu, W. Saad, M. Bennis, M. Debbah, and Z. Han, "Matching theory for future wireless networks: Fundamentals and applications," *IEEE Commun. Mag.*, vol. 53, no. 5, pp. 52–59, May 2015.

[14] B. Di, L. Song, and Y. Li, "Sub-channel assignment, power allocation, and user scheduling for non-orthogonal multiple access networks," *IEEE Trans. Wireless Commun.*, vol. 15, no. 11, pp. 7686–7698, Nov. 2016.

[15] J. Kang et al., "Optimizing task assignment for reliable blockchain-empowered federated edge learning," *IEEE Trans. Veh. Technol.*, vol. 70, no. 2, pp. 1910–1923, Feb. 2021.

[16] H. Du, D. Niyato, Y.-A. Xie, Y. Cheng, J. Kang, and D. In Kim, "Performance analysis and optimization for jammer-aided multi-antenna UAV covert communication," 2022, *arXiv:2202.00973*.

[17] F. Boccardi et al., "Why to decouple the uplink and downlink in cellular networks and how to do it," *IEEE Commun. Mag.*, vol. 54, no. 3, pp. 110–117, Mar. 2016.

[18] K. Yu, H. Zhou, Z. Tang, X. Shen, and F. Hou, "Deep reinforcement learning-based RAN slicing for UL/DL decoupled cellular V2X," *IEEE Trans. Wireless Commun.*, vol. 21, no. 5, pp. 3523–3535, May 2022.

[19] S. Singh, X. Zhang, and J. G. Andrews, "Joint rate and SINR coverage analysis for decoupled uplink-downlink biased cell associations in HetNets," *IEEE Trans. Wireless Commun.*, vol. 14, no. 10, pp. 5360–5373, Oct. 2015.

[20] K. Sun, J. Wu, W. Huang, H. Zhang, H.-Y. Hsieh, and V. C. M. Leung, "Uplink performance improvement for downlink-uplink decoupled HetNets with non-uniform user distribution," *IEEE Trans. Veh. Technol.*, vol. 69, no. 7, pp. 7518–7530, Jul. 2020.

[21] S. Yang and L. Hanzo, "Fifty years of MIMO detection: The road to large-scale MIMOs," *IEEE Commun. Surveys Tuts.*, vol. 17, no. 4, pp. 1941–1988, 4th Quart., 2015.

[22] Z. Jiang, S. Zhou, and Z. Niu, "Optimal antenna cluster size in cell-free large-scale distributed antenna systems with imperfect CSI and intercluster interference," *IEEE Trans. Veh. Technol.*, vol. 64, no. 7, pp. 2834–2845, Jul. 2015.

[23] G. Caire, N. Jindal, M. Kobayashi, and N. Ravindran, "Multiuser MIMO achievable rates with downlink training and channel state feedback," *IEEE Trans. Inf. Theory*, vol. 56, no. 6, pp. 2845–2866, Jun. 2010.

[24] E. A. Jorswieck, "Stable matchings for resource allocation in wireless networks," in *Proc. 17th Int. Conf. Digit. Signal Process. (DSP)*, Jul. 2011, pp. 1–8.

[25] K. Shen and W. Yu, "Fractional programming for communication systems—Part II: Uplink scheduling via matching," *IEEE Trans. Signal Process.*, vol. 66, no. 10, pp. 2631–2644, May 2018.

[26] Y. Gu, Y. Zhang, M. Pan, and Z. Han, "Matching and cheating in device to device communications underlying cellular networks," *IEEE J. Sel. Areas Commun.*, vol. 33, no. 10, pp. 2156–2166, Oct. 2015.

[27] J. Zhao, Y. Liu, K. K. Chai, Y. Chen, and M. Elkashlan, "Many-to-many matching with externalities for device-to-device communications," *IEEE Wireless Commun. Lett.*, vol. 6, no. 1, pp. 138–141, Feb. 2017.

[28] M. Simsek, T. Hößler, E. Jorswieck, H. Klessig, and G. Fettweis, "Multiconnectivity in multicellular, multiuser systems: A Matching-based approach," *Proc. IEEE*, vol. 107, no. 2, pp. 394–413, Feb. 2019.

[29] Q. Shi, M. Razaviyayn, Z.-Q. Luo, and C. He, "An iteratively weighted MMSE approach to distributed sum-utility maximization for a MIMO interfering broadcast channel," *IEEE Trans. Signal Process.*, vol. 59, no. 9, pp. 4331–4340, Sep. 2011.

[30] K. Shen and W. Yu, "Fractional programming for communication systems—Part I: Power control and beamforming," *IEEE Trans. Signal Process.*, vol. 66, no. 10, pp. 2616–2630, May 2018.

[31] K. Hosseini, W. Yu, and R. S. Adve, "Large-scale MIMO versus network MIMO for multicell interference mitigation," *IEEE J. Sel. Topics Signal Process.*, vol. 8, no. 5, pp. 930–941, Oct. 2014.

[32] H. Q. Ngo, A. Ashikhmin, H. Yang, E. G. Larsson, and T. L. Marzetta, "Cell-free massive MIMO versus small cells," *IEEE Trans. Wireless Commun.*, vol. 16, no. 3, pp. 1834–1850, Mar. 2017.

[33] H. A. Ammar, R. Adve, S. Shahbazpanahi, G. Boudreau, and K. V. Srinivas, "Downlink resource allocation in multiuser cell-free MIMO networks with user-centric clustering," *IEEE Trans. Wireless Commun.*, vol. 21, no. 3, pp. 1482–1497, Mar. 2022.

[34] Y. Zhao, W. Zhao, G. Wang, B. Ai, H. H. Putra, and B. Juliyanto, "AoA-based channel estimation for massive MIMO OFDM communication systems on high speed rails," *China Commun.*, vol. 17, no. 3, pp. 90–100, Mar. 2020.

[35] E. Björnson and L. Sanguinetti, "Making cell-free massive MIMO competitive with MMSE processing and centralized implementation," *IEEE Trans. Wireless Commun.*, vol. 19, no. 1, pp. 77–90, Jan. 2020.
[36] E. Bodine-Baron, C. Lee, A. Chong, B. Hassibi, and A. Wierman, "Peer effects and stability in matching markets," in *Proc. Int. Symp. Algorithmic Game Theory*. Cham, Switzerland: Springer, 2011, pp. 117–129.
[37] U. Kamecke, "Two sided matching: A study in game-theoretic modeling and analysis," vol. 59, no. 236, pp. 487–489, Nov. 1992.
[38] S. Jaeckel, L. Raschkowski, K. Börner, and L. Thiele, "QuaDRiGa: A 3-D multi-cell channel model with time evolution for enabling virtual field trials," *IEEE Trans. Antennas Propag.*, vol. 62, no. 6, pp. 3242–3256, Jun. 2014, doi: 10.1109/TAP.2014.2310220.

Kai Yu (Student Member, IEEE) received the B.S. degree in detection, guidance, and control technology from the University of Electronic Science and Technology of China, Chengdu, China, in 2019. He is currently pursuing the Ph.D. degree with the School of Electronic Science and Engineering, Nanjing University, China. His research interests include resource allocation, machine learning for wireless communications, and heterogeneous networks.

Quan Yu (Fellow, IEEE) received the Ph.D. degree in fiber optics from the University of Limoges in 1992. In 1992, he joined the Faculty of the Institute of China Electronic System Engineering Corporation. He is currently a Principal Research Scientist with the Peng Cheng Laboratory. His main areas of research interest are the architecture of wireless networks, optimization of protocols, and cognitive radios. He is an Academician of the Chinese Academy of Engineering (CAE). He is the Founding Editor-in-Chief of the *Journal of Communications and Information Networks*.

Zhixuan Tang (Student Member, IEEE) received the B.S. degree in communication engineering from Nanjing University, Nanjing, China, in 2020, where she is currently pursuing the M.S. degree with the School of Electronic Science and Engineering. She mainly focuses on the dynamic resource management and networking optimization in the field of emerging wireless networks.

Jiwei Zhao (Member, IEEE) received the M.S. degree in information and communication system from Xidian University, Xi'an, China, in 2018. He is currently pursuing the Ph.D. degree with the School of Electronic Science and Engineering, Nanjing University, Nanjing, China. His research interests include fully-decoupled RAN architecture, coordinated multi-point, and machine learning applications for wireless communication. He has won the first prize in the 2016 CCF (China Computer Federation) China Big Data and Cloud Computing Intelligence Contest.

Bo Qian (Member, IEEE) received the B.S. and M.S. degrees in statistics from Sichuan University, Chengdu, China, in 2015 and 2018, respectively, and the Ph.D. degree in information and communication engineering from Nanjing University, Nanjing, China, in 2022. He is currently a Post-Doctoral Fellow with the Peng Cheng Laboratory, Shenzhen, China. His research interests include resource management in B5G/6G networks, VANET, network economics, blockchain, and game theory. He was a recipient of the Best Paper Award from IEEE VTC2020-Fall.

Yunting Xu (Student Member, IEEE) received the B.S. degree in communication engineering from Nanjing University, Nanjing, China, in 2017, where he is currently pursuing the Ph.D. degree with the School of Electronic Science and Engineering. He mainly focuses on the wireless network access, dynamic resource management, and personalized wireless service in the field of next generation wireless networks.

Haibo Zhou (Senior Member, IEEE) received the Ph.D. degree in information and communication engineering from Shanghai Jiao Tong University, Shanghai, China, in 2014. From 2014 to 2017, he was a Post-Doctoral Fellow with the Broadband Communications Research Group, Department of Electrical and Computer Engineering, University of Waterloo. He is currently a Full Professor with the School of Electronic Science and Engineering, Nanjing University, Nanjing, China. His research interests include resource management and protocol design in B5G/6G networks, vehicular ad hoc networks, and space-air-ground integrated networks. He was a recipient of the 2019 IEEE ComSoc Asia–Pacific Outstanding Young Researcher Award. He served as a Track Co-Chair/a Symposium Co-Chair for IEEE/CIC ICCC 2019, IEEE VTC-Fall 2020, IEEE VTC-Fall 2021, and IEEE GLOBECOM 2022. He is currently an Associate Editor of the IEEE TRANSACTIONS ON WIRELESS COMMUNICATIONS, IEEE INTERNET OF THINGS JOURNAL, *IEEE Network Magazine*, and IEEE WIRELESS COMMUNICATIONS LETTER.

Xuemin (Sherman) Shen (Fellow, IEEE) received the Ph.D. degree in electrical engineering from Rutgers University, New Brunswick, NJ, USA, in 1990. He is a University Professor with the Department of Electrical and Computer Engineering, University of Waterloo, Canada. His research focuses on network resource management, wireless network security, the Internet of Things, 5G and beyond, and vehicular ad hoc and sensor networks.

He is a registered Professional Engineer of Ontario, Canada. He is an Engineering Institute of Canada fellow, a Canadian Academy of Engineering fellow, a Royal Society of Canada fellow, and a Chinese Academy of Engineering Foreign Member. He received the Canadian Award for Telecommunications Research from the Canadian Society of Information Theory (CSIT) in 2021, the R. A. Fessenden Award in 2019 from IEEE, Canada, the Award of Merit from the Federation of Chinese Canadian Professionals (Ontario) in 2019, the James Evans Avant Garde Award in 2018 from the IEEE Vehicular Technology Society, the Joseph LoCicero Award in 2015 and the Education Award in 2017 from the IEEE Communications Society, and the Technical Recognition Award from the Wireless Communications Technical Committee (2019) and the AHSN Technical Committee (2013). He has also received the Excellent Graduate Supervision Award in 2006 from the University of Waterloo and the Premiers Research Excellence Award (PREA) in 2003 from the Province of Ontario, Canada. He served as the Technical Program Committee Chair/the Co-Chair for IEEE Globecom16, IEEE Infocom14, IEEE VTC10 Fall, and IEEE Globecom07; and the Chair for the IEEE Communications Society Technical Committee on Wireless Communications. He is the President of the IEEE Communications Society. He was the Vice President of technical and educational activities, a Vice President of publications, Member-at-Large on the Board of Governors, the Chair of the Distinguished Lecturer Selection Committee, and a member of IEEE Fellow Selection Committee of the ComSoc. He served as the Editor-in-Chief for the IEEE INTERNET OF THINGS JOURNAL, IEEE NETWORK, and *IET Communications*. He is a Distinguished Lecturer of the IEEE Vehicular Technology Society and Communications Society.